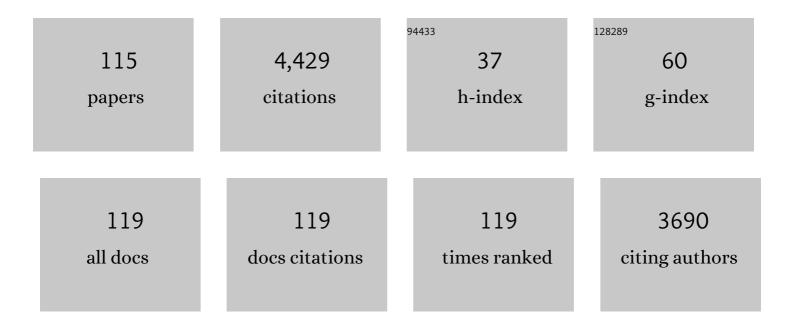
List of Publications by Year in descending order

Source: https://exaly.com/author-pdf/1985029/publications.pdf Version: 2024-02-01



LUAN LUU

#	Article	IF	CITATIONS
1	Stable isotope fractionation of thallium as novel evidence for its geochemical transfer during lead‑zinc smelting activities. Science of the Total Environment, 2022, 803, 150036.	8.0	16
2	Microbial response and adaption to thallium contamination in soil profiles. Journal of Hazardous Materials, 2022, 423, 127080.	12.4	37
3	Quantification of smelter-derived contributions to thallium contamination in river sediments: Novel insights from thallium isotope evidence. Journal of Hazardous Materials, 2022, 424, 127594.	12.4	17
4	Associations between prenatal multiple metal exposure and preterm birth: Comparison of four statistical models. Chemosphere, 2022, 289, 133015.	8.2	13
5	Simultaneous Electrochemical Detection of Co-Existing Dihydroxybenzene Isomers Using Porphyrin Zr Metal-Organic Frameworks/β-cyclodextrin/Pencil Graphite Electrode. IEEE Sensors Journal, 2022, 22, 2993-3000.	4.7	3
6	Effect of electric field on the microstructure and electrical properties of (In + Ta) co-doped TiO2 colossal dielectric ceramics. Journal of Materials Science: Materials in Electronics, 2022, 33, 6283-6293.	2.2	16
7	Singlemode-Multimode-Singlemode Optical Fiber Sensor for Accurate Blood Pressure Monitoring. Journal of Lightwave Technology, 2022, 40, 4443-4450.	4.6	13
8	Synergetic removal of thallium and antimony from wastewater with jacobsite-biochar-persulfate system. Environmental Pollution, 2022, 304, 119196.	7.5	12
9	Thallium isotopic compositions as tracers in environmental studies: A review. Environment International, 2022, 162, 107148.	10.0	15
10	Effect of IncRNA MALAT1 on the Granulosa Cell Proliferation and Pregnancy Outcome in Patients With PCOS. Frontiers in Endocrinology, 2022, 13, 825431.	3.5	7
11	Controllable low-temperature flash sintering and giant dielectric performance of (Zn, Ta) co-doped TiO2 ceramics. Ceramics International, 2022, 48, 24629-24637.	4.8	14
12	SunUp and Sunset genomes revealed impact of particle bombardment mediated transformation and domestication history in papaya. Nature Genetics, 2022, 54, 715-724.	21.4	26
13	Associations of benzotriazoles and benzothiazoles with estrogens and androgens among pregnant women: A cohort study with repeated measurements. Science of the Total Environment, 2022, 838, 155998.	8.0	3
14	Dielectric, ferroelectric and magnetic properties of Bi(Mg,M)O3-modified (M=Hf, Ta) BiFeO3–BaTiO3 ceramics. Journal of Materials Science: Materials in Electronics, 2022, 33, 17174-17189.	2.2	5
15	Flash sintering preparation and colossal dielectric origin of (Al0.5Ta0.5)0.05Ti0.95O2 ceramics. Journal of Materials Science: Materials in Electronics, 2022, 33, 15802-15813.	2.2	5
16	Effects of the electric field on microstructure and electrical properties of ZnO–Bi2O3–Co2O3 varistor by flash sintering. Journal of Materials Science: Materials in Electronics, 2022, 33, 17900-17911.	2.2	5
17	Giant dielectric permittivity of Ca and Sb-co-doped TiO2 ceramics. Journal of Materials Science: Materials in Electronics, 2022, 33, 18389-18399.	2.2	2
18	Highly efficient removal of thallium in wastewater by MnFe2O4-biochar composite. Journal of Hazardous Materials, 2021, 401, 123311.	12.4	142

#	Article	IF	CITATIONS
19	Mach-Zehnder Interferometer for High Temperature (1000 °C) Sensing Based on a Few-Mode Fiber. Photonic Sensors, 2021, 11, 341-349.	5.0	12
20	Emerging risks of toxic metal(loid)s in soil-vegetables influenced by steel-making activities and isotopic source apportionment. Environment International, 2021, 146, 106207.	10.0	105
21	Emergent thallium exposure from uranium mill tailings. Journal of Hazardous Materials, 2021, 407, 124402.	12.4	71
22	Effect of transition metal element substitution on magnetoelectric properties of BiFeO3-BaTiO3 ceramics. Journal of Alloys and Compounds, 2021, 859, 158224.	5.5	14
23	Reproductive potential of mosquitofish is reduced by the masculinizing effect of a synthetic progesterone, gestodene: Evidence from morphology, courtship behaviour, ovary histology, sex hormones and gene expressions. Science of the Total Environment, 2021, 769, 144570.	8.0	13
24	Distribution and migration characteristics of dinitrotoluene sulfonates (DNTs) in typical TNT production sites: Effects and health risk assessment. Journal of Environmental Management, 2021, 287, 112342.	7.8	9
25	The phenylalanine ammonia-lyase gene McPAL3: the key gene involved in the scopoletin accumulation of MorindaÂcitrifolia L Revista Brasileira De Botanica, 2021, 44, 663-670.	1.3	1
26	Cadmium isotopic fractionation in lead-zinc smelting process and signatures in fluvial sediments. Journal of Hazardous Materials, 2021, 411, 125015.	12.4	45
27	Geochemical and U-Th isotopic insights on uranium enrichment in reservoir sediments. Journal of Hazardous Materials, 2021, 414, 125466.	12.4	40
28	Sex biased expression of hormone related genes at early stage of sex differentiation in papaya flowers. Horticulture Research, 2021, 8, 147.	6.3	12
29	Adsorption Force of Fibronectin: A Balance Regulator to Transmission of Cell Traction Force and Fluid Shear Stress. Biomacromolecules, 2021, 22, 3264-3273.	5.4	5
30	A combined management scheme to simultaneously mitigate As and Cd concentrations in rice cultivated in contaminated paddy soil. Journal of Hazardous Materials, 2021, 416, 125837.	12.4	35
31	Uranium re-adsorption on uranium mill tailings and environmental implications. Journal of Hazardous Materials, 2021, 416, 126153.	12.4	51
32	New insights into ball milling effects on MgAl-LDHs exfoliation on biochar support: A case study for cadmium adsorption. Journal of Hazardous Materials, 2021, 416, 126258.	12.4	46
33	A current-controlled flash sintering processing leading to dense and fine-grained typical multi-element ZnO varistor ceramics. Journal of Alloys and Compounds, 2021, 876, 160124.	5.5	20
34	Integrating disulfides into a polyethylenimine gene carrier selectively boosts significant transfection activity in lung tissue enabling robust IL-12 gene therapy against metastatic lung cancers. Materials Science and Engineering C, 2021, 128, 112358.	7.3	3
35	Advances in the chemistry, pharmacological diversity, and metabolism of 20(R)-ginseng saponins. Journal of Ginseng Research, 2020, 44, 14-23.	5.7	42
36	Geochemical fractionation of thallium in contaminated soils near a large-scale Hg-Tl mineralised area. Chemosphere, 2020, 239, 124775.	8.2	32

#	Article	IF	CITATIONS
37	Enhancement of dielectric and non-ohmic properties of graded Co doped CaCu3Ti4O12 thin films. Journal of Alloys and Compounds, 2020, 816, 152582.	5.5	32
38	Thallium isotopic fractionation in industrial process of pyrite smelting and environmental implications. Journal of Hazardous Materials, 2020, 384, 121378.	12.4	73
39	The regulatory mechanism of Chryseobacterium sp. resistance mediated by montmorillonite upon cadmium stress. Chemosphere, 2020, 240, 124851.	8.2	27
40	Processing and characterizations of flash sintered ZnO-Bi2O3-MnO2 varistor ceramics under different electric fields. Journal of the European Ceramic Society, 2020, 40, 1330-1337.	5.7	35
41	Temporal sedimentary record of thallium pollution in an urban lake: An emerging thallium pollution source from copper metallurgy. Chemosphere, 2020, 242, 125172.	8.2	73
42	The role of cis-elements in the evolution of crassulacean acid metabolism photosynthesis. Horticulture Research, 2020, 7, 5.	6.3	19
43	Thallium contamination, health risk assessment and source apportionment in common vegetables. Science of the Total Environment, 2020, 703, 135547.	8.0	73
44	Hyperaccumulation and transport mechanism of thallium and arsenic in brake ferns (Pteris vittata L.): A case study from mining area. Journal of Hazardous Materials, 2020, 388, 121756.	12.4	58
45	Health risks of metal(loid)s in maize (Zea mays L.) in an artisanal zinc smelting zone and source fingerprinting by lead isotope. Science of the Total Environment, 2020, 742, 140321.	8.0	39
46	Fabrication and electrical characteristics of flash-sintered SiO2-doped ZnO-Bi2O3-MnO2 varistors. Journal of Advanced Ceramics, 2020, 9, 683-692.	17.4	53
47	Quantitative isotopic fingerprinting of thallium associated with potentially toxic elements (PTEs) in fluvial sediment cores with multiple anthropogenic sources. Environmental Pollution, 2020, 266, 115252.	7.5	30
48	Persistent thallium contamination in river sediments, source apportionment and environmental implications. Ecotoxicology and Environmental Safety, 2020, 202, 110874.	6.0	28
49	Microbial insights into the biogeochemical features of thallium occurrence: A case study from polluted river sediments. Science of the Total Environment, 2020, 739, 139957.	8.0	58
50	Effect of tuning A/B substitutions on multiferroic characteristics of BiFeO3-based ternary system ceramics. Journal of Magnetism and Magnetic Materials, 2020, 510, 166928.	2.3	16
51	Flash sintering preparation and electrical properties of ZnO–Bi2O3-M (M = Cr2O3, MnO2 or Co2O3) varistor ceramics. Ceramics International, 2020, 46, 14913-14918.	4.8	27
52	Colossal permittivity characteristics and mechanism of (Sr, Ta) co-doped TiO2 ceramics. Journal of Materials Science: Materials in Electronics, 2020, 31, 5205-5213.	2.2	22
53	Critical insight and indication on particle size effects towards uranium release from uranium mill tailings: Geochemical and mineralogical aspects. Chemosphere, 2020, 250, 126315.	8.2	37
54	Legacy of multiple heavy metal(loid)s contamination and ecological risks in farmland soils from a historical artisanal zinc smelting area. Science of the Total Environment, 2020, 720, 137541.	8.0	104

#	Article	IF	CITATIONS
55	Effects and mechanisms of mineral amendment on thallium mobility in highly contaminated soils. Journal of Environmental Management, 2020, 262, 110251.	7.8	27
56	Multifunctional magnetic MgMn-oxide composite for efficient purification of Cd2+ and paracetamol pollution: Synergetic effect and stability. Journal of Hazardous Materials, 2020, 388, 122078.	12.4	41
57	Structure, ferroelectric and magnetic characteristics of SmFeO3 and BaTiO3 co-modified BiFeO3 ceramics. Journal of Materials Science: Materials in Electronics, 2020, 31, 3479-3491.	2.2	6

Effect of ionic radius on colossal permittivity properties of (A, Ta) co-doped TiO2 (A= alkaline-earth) Tj ETQq0 0 0 rg $\frac{BT}{4.8}$ /Overlock 10 Tf 5

59	Enantioselective synthesis of chiral α-alkynylated thiazolidones by tandem S-addition/acetalization of alkynyl imines. Organic and Biomolecular Chemistry, 2020, 18, 3117-3124.	2.8	8
60	Norethindrone alters mating behaviors, ovary histology, hormone production and transcriptional expression of steroidogenic genes in zebrafish (Danio rerio). Ecotoxicology and Environmental Safety, 2020, 195, 110496.	6.0	11
61	Geochemical transfer of cadmium in river sediments near a lead-zinc smelter. Ecotoxicology and Environmental Safety, 2020, 196, 110529.	6.0	82
62	Cadmium isotopes as tracers in environmental studies: A review. Science of the Total Environment, 2020, 736, 139585.	8.0	66
63	Mechanisms of U(VI) removal by biochar derived from Ficus microcarpa aerial root: A comparison between raw and modified biochar. Science of the Total Environment, 2019, 697, 134115.	8.0	78
64	The bracteatus pineapple genome and domestication of clonally propagated crops. Nature Genetics, 2019, 51, 1549-1558.	21.4	60
65	High contamination risks of thallium and associated metal(loid)s in fluvial sediments from a steel-making area and implications for environmental management. Journal of Environmental Management, 2019, 250, 109513.	7.8	43
66	Transcriptomic and physiological changes in western mosquitofish (Gambusia affinis) after exposure to norgestrel. Ecotoxicology and Environmental Safety, 2019, 171, 579-586.	6.0	10
67	Three-Dimensional Printing of Biodegradable Piperazine-Based Polyurethane-Urea Scaffolds with Enhanced Osteogenesis for Bone Regeneration. ACS Applied Materials & Interfaces, 2019, 11, 9415-9424.	8.0	51
68	Exploring the mechanisms of organic matter degradation and methane emission during sewage sludge composting with added vesuvianite: Insights into the prediction of microbial metabolic function and enzymatic activity. Bioresource Technology, 2019, 286, 121397.	9.6	76
69	Thallium pollution in China and removal technologies for waters: A review. Environment International, 2019, 126, 771-790.	10.0	180
70	Thallium contamination in farmlands and common vegetables in a pyrite mining city and potential health risks. Environmental Pollution, 2019, 248, 906-915.	7.5	122
71	Response of microbial communities and interactions to thallium in contaminated sediments near a pyrite mining area. Environmental Pollution, 2019, 248, 916-928.	7.5	70
72	Dissolution Behavior of Isolated and Aggregated Hematite Particles Revealed by in Situ Liquid Cell Transmission Electron Microscopy. Environmental Science & Technology, 2019, 53, 2416-2425.	10.0	20

5

#	Article	IF	CITATIONS
73	Beneficial influences of pelelith and dicyandiamide on gaseous emissions and the fungal community during sewage sludge composting. Environmental Science and Pollution Research, 2019, 26, 8928-8938.	5.3	25
74	GraphConvLSTM: Spatiotemporal Learning for Activity Recognition with Wearable Sensors. , 2019, , .		6
75	The mobility of thallium in sediments and source apportionment by lead isotopes. Chemosphere, 2019, 219, 864-874.	8.2	56
76	Rapid masculinization and effects on the liver of female western mosquitofish (Gambusia affinis) by norethindrone. Chemosphere, 2019, 216, 94-102.	8.2	20
77	Adsorption of thallium(I) on rutile nano-titanium dioxide and environmental implications. PeerJ, 2019, 7, e6820.	2.0	8
78	A Novel Roomâ€Temperature Multiferroic System of Hexagonal Lu _{1â^'} <i>_x</i> In <i>_x</i> FeO ₃ . Advanced Functional Materials, 2018, 28, 1706062.	14.9	34
79	Papain-like cysteine proteases in Carica papaya: lineage-specific gene duplication and expansion. BMC Genomics, 2018, 19, 26.	2.8	28
80	Structural effects on the catalytic activity of carbon-supported magnetite nanocomposites in heterogeneous Fenton-like reactions. RSC Advances, 2018, 8, 16193-16201.	3.6	14
81	Provenance of uranium in a sediment core from a natural reservoir, South China: Application of Pb stable isotope analysis. Chemosphere, 2018, 193, 1172-1180.	8.2	35
82	Androgen-induced alterations in endometrial proteins crucial in recurrent miscarriages. Oncotarget, 2018, 9, 24627-24641.	1.8	15
83	Two Kinds of Novel Multi-user Immersive Display Systems. , 2018, , .		6
84	Allele-defined genome of the autopolyploid sugarcane Saccharum spontaneum L Nature Genetics, 2018, 50, 1565-1573.	21.4	463
85	Emerging Thallium Pollution in China and Source Tracing by Thallium Isotopes. Environmental Science & Technology, 2018, 52, 11977-11979.	10.0	52
86	Reversible Fe(<scp>ii</scp>) uptake/release by magnetite nanoparticles. Environmental Science: Nano, 2018, 5, 1545-1555.	4.3	20
87	Thallium contamination in arable soils and vegetables around a steel plant—A newly-found significant source of Tl pollution in South China. Environmental Pollution, 2017, 224, 445-453.	7.5	131
88	Discovery, semisynthesis, biological activities, and metabolism of ocotillol-type saponins. Journal of Ginseng Research, 2017, 41, 373-378.	5.7	60
89	Ferroelectric and magnetic properties in (1Ⱂ <i>x</i>)BiFeO ₃ – <i>x</i> (0.5CaTiO ₃ –0.5SmFeO ₃) ceramics. Journal of the American Ceramic Society, 2017, 100, 4045-4057.	3.8	24
90	Incorporating isosorbide as the chain extender improves mechanical properties of linear biodegradable polyurethanes as potential bone regeneration materials. RSC Advances, 2017, 7, 13886-13895.	3.6	20

#	Article	IF	CITATIONS
91	Enhanced photocurrent production by the synergy of hematite nanowire-arrayed photoanode and bioengineered Shewanella oneidensis MR-1. Biosensors and Bioelectronics, 2017, 94, 227-234.	10.1	57
92	Chiral Primary Amine Catalysis for Asymmetric Mannich Reactions of Aldehydes with Ketimines: Stereoselectivity and Reactivity. Angewandte Chemie - International Edition, 2017, 56, 12697-12701.	13.8	67
93	Chiral Primary Amine Catalysis for Asymmetric Mannich Reactions of Aldehydes with Ketimines: Stereoselectivity and Reactivity. Angewandte Chemie, 2017, 129, 12871-12875.	2.0	15
94	Synthesis and crystal structures of a 3-acetylated (20 <i>S</i> ,24 <i>S</i>)-ocotillol-type saponin and its C-24 epimer. Acta Crystallographica Section C, Structural Chemistry, 2017, 73, 464-469.	0.5	8
95	Effect of (Sr0.7Ca0.3)TiO3-substitution on structure, dielectric, ferroelectric, and magnetic properties of BiFeO3 ceramics. Journal of Applied Physics, 2016, 119, .	2.5	23
96	Thallium transformation and partitioning during Pb–Zn smelting and environmental implications. Environmental Pollution, 2016, 212, 77-89.	7.5	78
97	Preliminary results of spatial distribution of uranium and thorium in soil profiles near a uranium industrial site, Guangdong province, China. Nukleonika, 2016, 61, 367-371.	0.8	11
98	Aggregation Kinetics of Hematite Particles in the Presence of Outer Membrane Cytochrome OmcA of <i>Shewanella oneidenesis</i> MR-1. Environmental Science & Technology, 2016, 50, 11016-11024.	10.0	53
99	Technologically elevated natural radioactivity and assessment of dose to workers around a granitic uranium deposit area, China. Journal of Radioanalytical and Nuclear Chemistry, 2016, 310, 733-741.	1.5	17
100	Thallium dispersal and contamination in surface sediments from South China and its source identification. Environmental Pollution, 2016, 213, 878-887.	7.5	44
101	Synthesis and crystal structures of C24-epimeric 20(<i>R</i>)-ocotillol-type saponins. Acta Crystallographica Section C, Structural Chemistry, 2016, 72, 498-503.	0.5	13
102	Surface Sediment Contamination by Uranium Mining/Milling Activities in South China. Clean - Soil, Air, Water, 2015, 43, 414-420.	1.1	24
103	Significantly enhanced ferroelectricity and magnetic properties in (Sr0.5Ca0.5)TiO3-modified BiFeO3 ceramics. Journal of Applied Physics, 2015, 117, 174101.	2.5	12
104	Laser pulse compression method to measure Brillouin gain in water. Journal of Modern Optics, 2015, 62, 877-882.	1.3	0
105	Experimental and model studies on comparison of As(III and V) removal from synthetic acid mine drainage by bone char. Mineralogical Magazine, 2014, 78, 73-89.	1.4	12
106	Cross Regulation Between cGMP-dependent Protein Kinase and Akt in Vasodilatation of Porcine Pulmonary Artery. Journal of Cardiovascular Pharmacology, 2014, 64, 452-459.	1.9	5
107	Quick sulfide buffering in inner shelf sediments of the East China Sea impacted by eutrophication. Environmental Earth Sciences, 2014, 71, 465-473.	2.7	11
108	Adsorption of arsenic(V) on bone char: batch, column and modeling studies. Environmental Earth Sciences, 2014, 72, 2081-2090.	2.7	32

#	Article	IF	CITATIONS
109	The vibration characterization of synthetic crystalline lead hydrogen arsenite chloride precipitates Pb2(HAsO3)Cl2-implications of solidification of As (III) and Pb (II). Spectrochimica Acta - Part A: Molecular and Biomolecular Spectroscopy, 2014, 117, 658-661.	3.9	2
110	Environmental exposure and flux of thallium by industrial activities utilizing thallium-bearing pyrite. Science China Earth Sciences, 2013, 56, 1502-1509.	5.2	24
111	Surface Water Contamination by Uranium Mining/Milling Activities in Northern Guangdong Province, China. Clean - Soil, Air, Water, 2012, 40, 1357-1363.	1.1	35
112	Primary and repetitive secondary somatic embryogenesis in Rosa hybrida â€~Samantha'. Plant Cell, Tissue and Organ Culture, 2012, 109, 411-418.	2.3	33
113	Sorption of thallium(I) onto geological materials: Influence of pH and humic matter. Chemosphere, 2011, 82, 866-871.	8.2	58
114	Comparative characterization of two natural humic acids in the Pearl River Basin, China and their environmental implications. Journal of Environmental Sciences, 2010, 22, 1695-1702.	6.1	14
115	Thallium Distribution in Sediments from the Pearl River Basin, China. Clean - Soil, Air, Water, 2010, 38, 909-915.	1.1	32